JOURNAL OF AIRCRAFT
Vol. 31, No. 4, July–Aug. 1994

# Analytic Sensitivities for Shape Optimization in Equivalent Plate Structural Wing Models

Eli Livne*
*University of Washington, Seattle, Washington 98195*

**Equivalent plate modeling techniques based on Ritz analysis with simple polynomials prove to be efficient tools for structural modeling of wings in the preliminary design stage. Accuracy problems are encountered, however, when these models are used to obtain finite difference behavior sensitivities with respect to planform shape. The accuracy problems are associated with the poor numerical conditioning of static and eigenvalue equations. As higher-order polynomials are being used to improve the analysis itself, the more sensitive is the finite difference derivative to the step size used. This article describes a formulation of wing equivalent plate modeling in which it is simple to obtain analytic, explicit expressions for stiffness and mass matrix elements without the need to perform numerical integration. This formulation leads naturally to analytic expressions for the derivatives of displacements, stresses, and natural frequencies with respect to shape design variables. This article examines the accuracy of finite difference derivatives compared with the analytic derivatives, and shows that in some cases it is impossible to obtain any information of value by finite differences. Analytic sensitivities, in this case, are still sufficiently accurate for design optimization.**

## Nomenclature

$A^R$ = cross-sectional area of rib
$A_1^R$, $A_2^R$ = coefficients of the linear cross-sectional area of a rib
$A^S$ = cross-sectional area of spar
$A_1^S$, $A_2^S$ = coefficients of linear cross-sectional area of a spar
$a_1$, $a_2$ = coefficients of the aft line defining a trapezoid in the $x$-$y$ plane
$[F]$, $[G]$ = matrices relating the coordinates of the vertices of a wing trapezoid to position of grid points of the deforming mesh, defined in Eqs. (37–41)
$f_1$, $f_2$ = coefficients of the front line defining a trapezoid in the $x$-$y$ plane
$H(ih)$ = $ih$th coefficient in the polynomial series for wing depth
$h(x, y)$ = wing depth distribution
$I_A$, $I_F$ = line integrals along the aft and front lines of a wing trapezoid, Eqs. (28) and (29)
$I_{RB}$ = line integral of a polynomial term over a rib
$I_{SP}$ = line integral of a polynomial term over a spar
$I_{TR}$ = area integral of a polynomial term over a trapezoid
$[K]$, $K(i, j)$ = stiffness matrix and its $i$, $j$th term
$MW(k, l)$, $NW(k, l)$ = $x$ and $y$ powers in the polynomial $k$, $l$ term of $[W]$
$mh(ih)$, $nh(ih)$ = $ih$th powers of $x$ and $y$ in the polynomial series for wing depth
$mt(il, it)$, $nt(il, it)$ = $it$th powers of $x$ and $y$ in the polynomial series for the thickness of the $il$th skin layer
$mw(iw)$, $nw(iw)$ = $x$ and $y$ powers in the polynomial Ritz series for the vertical displacement $w(x, y)$
$N_l$ = number of skin layers
$N_q$, $n_q$ = number of terms in the Ritz series for $w(x, y)$
$PE$ = strain energy
$[Q^{il}]$ = constitutive material matrix ($3 \times 3$) for the $il$th skin layer
$\{q\}$ = vector of generalized displacements
$S_1$, $S_2$ = coefficients of a spar line in the $x$, $y$ plane
$T_{(il,it)}$ = the $it$th coefficient in the polynomial series for the thickness of the $il$th layer
$t_{il}(x, y)$ = thickness of the $il$th skin layer
$\{U\}^T$ = displacement vector, $\{u, v, w\}$
$[W(x, y)]$ = $3 \times nq$, a matrix of polynomial terms relating the curvatures to generalized displacements
$\bar{W}(k, l)$ = coefficient of the $k$, $l$ term of matrix $[W]$
$x_A$, $x_F$ = aft and forward $x$ coordinates of rib edges
$x_{FL}$, $x_{FR}$, $x_{AL}$, $x_{AR}$ = $x$ coordinates of the vertices of a wing trapezoid (from front-left to aft-right)
$\{x^{OP}\}$ = vector of shape design variables defining a wing trapezoid
$xf(y)$, $xa(y)$ = equations for the front and aft lines defining a trapezoid in the $x$-$y$ plane
$y_L$, $y_R$ = left and right spanwise coordinates of a trapezoid
$y_{RIB}$ = spanwise location of a rib
$\{\varepsilon\}$ = skin strain vector
$\{\sigma^{il}\}$ = stress vector for skin layer $il$

*Indices*
$ih$ = index of a term in the polynomial depth series

Received Feb. 25, 1993; revision received Sept. 16, 1993; accepted for publication Nov. 18, 1993. 

*Assistant Professor, Aeronautics and Astronautics. Senior Member AIAA.

$il$ = skin layer number
$it$ = index of a term in the polynomial series for a layer thickness
$jh$ = index of a term in the polynomial depth series

## Introduction

COMPARED to sizing structural optimization problems, shape optimization is more complex and more difficult to tackle.[1] Major difficulties are associated with accuracy problems in the finite difference calculation of sensitivity derivatives, the need to control mesh deformation, proper parameterization of structural shape, and a more time-consuming repeated generation of stiffness and mass matrices.

In the context of airplane preliminary design, as aerodynamic and structural characteristics of an evolving configuration change, optimization with respect to shape is essential. Yet, the automated preliminary design synthesis of wing structures, in which the wing planform shape is varied and control surfaces are sized and moved to their optimal locations, is still a challenge.

The equivalent plate approach for structural modeling of low aspect ratio thin wings was used in the TSO aeroelastic tailoring code.[2] Further improvements and generalizations in the equivalent laminated plate solution (ELAPS computer code, Refs. 3 and 4) made it into a powerful, efficient tool for wing structural analysis. Equivalent plate models were used for wing aeroelastic tailoring, optimization, parametric studies, and multidisciplinary synthesis.[5-12] What makes the equivalent plate approach desirable in the context of wing preliminary design and optimization are the ease and speed of data preparation for new configurations, the high computational efficiency, and the ease of manipulation of the Ritz displacement functions used. This last property makes it possible to avoid one of the classical problems of aeroelasticity—the transformation of data between the structural and aerodynamics grids. With equivalent plates, structural deformation is readily available for any set of aerodynamic grid points on the wing.

Equivalent plate models, however, as they stand today, need modification before their true potential can be realized for wing shape optimization. For effective, reliable behavior sensitivity analysis, the ability to calculate analytical derivatives with respect to shape as well as sizing-type design variables is important. This is even more important when the Ritz functions used are simple polynomials.[3,4,8,9] Simple polynomial Ritz functions lead to substantial saving in computing time. They also lead to numerical ill conditioning of the resulting equations when the order of polynomials is increased. Experience reported in Refs. 3 and 4 and confirmed later by other studies (Refs. 8 and 9), shows that useful analysis results can be obtained with an equivalent plate model based on simple polynomials before the static and dynamic solutions become ill conditioned.

ELAPS, however, was originally developed as an analysis tool only. Through the application of automatic differentation[11] (which can lead to codes for calculating analytical sensitivities), an analytic derivative capability was added recently to ELAPS. However, using finite differences for sensitivity calculation in the context of multidisciplinary optimization is still a widely used practice because of its ease of implementation. When analysis capabilities such as ELAPS are used to obtain behavior sensitivities by finite differences or by the semianalytic method,[13-16] the poor numerical conditioning can lead to large errors in the derivatives obtained—a problem that has not been discussed in any of the publications on equivalent plate wing modeling.

The lifting surface control augmented structural synthesis code (LS-CLASS[8,9]) was developed with the capability to obtain analytic behavior sensitivities with respect to sizing type design variables, but not with respect to shape variables. One recent development of analytical shape sensitivities for plates is described in Ref. 17. In that particular formulation orthogonal polynomials are used instead of simple polynomials as Ritz functions. This prevents ill conditioning, but also leads to an increase in computation time. Developments reported in Ref. 17 are still limited at this stage to panels. A method for obtaining analytical sensitivities with respect to shape is, then, needed for equivalent plate structural analysis of realistic wing structures. In addition, a careful examination of finite difference shape sensitivities is important and guidelines are needed for cases in which equivalent plate analysis tools are used to obtain behavior derivatives by finite differences.

This article describes a formulation of the equivalent plate approach that makes it possible to obtain analytic shape sensitivities of wing box structures (including their internal structures in the form of ribs and spars) in a simple manner. Detailed derivations of contributions from selected structural elements are used to illustrate important features of the numerical techniques used. It is shown how using simple polynomials as a basis for analysis leads to savings in terms of computing time and memory requirements not only for the analysis phase (as reported in Refs. 3 and 8), but also for shape sensitivity calculations. The resulting analytical shape sensitivities are used to evaluate accuracy of finite difference derivatives. It is shown that because of poor conditioning it is sometimes impossible to obtain accurate shape sensitivities based on finite differences, even when the analysis itself is still valid. Analytical sensitivities are the only reliable source of sensitivity information in those cases. If, nevertheless, only finite difference derivatives are available with certain applications, this article goes on to suggest a technique to alleviate the accuracy problems expected. In this context the convergence of behavior functions and their sensitivities are examined and provide guidance to potential users of the equivalent plate approach.

## Wing Box Geometry

A wing-tail configuration subject to planform shape changes is shown in Fig. 1. Lifting surfaces can move along the fuselage, change sweep, chord, and span. Spars and ribs can also move as the internal structural layout is changed. Lifting surfaces are made of collections of trapezoidal areas. A typical wing box trapezoid is shown in Fig. 2. Its planform shape is defined by its left and right spanwise coordinates $y_L$, $y_R$ and the $x$ coordinates of its four edges $x_{FL}$, $x_{FR}$, $x_{AL}$, $x_{AR}$. Its depth is defined by a simple polynomial in $x$ and $y$ of the form

$$h(x, y) = \sum_{ih=1}^{N_H} H(ih) x^{mh(ih)} y^{nh(ih)} \tag{1}$$

where $H(ih)$ are coefficients and $mh(ih)$, $nh(ih)$ are exponents of $x$ and $y$ terms in the polynomial series.

Figure 2 also shows spars and ribs in the trapezoid. Spar geometry is defined (in addition to the depth distribution $h(x, y)$ that determines cap vertical distance from the midplane) by four shape variables, namely the $(x, y)$ coordinates of the left and right edges $(sy_L, sx_L, sy_R, sx_R)$. Ribs (running parallel to the $x$ axis) are defined geometrically by three design variables each ($x_F$, $x_A$ and $y_{RIB}$), as shown.

The skins are made of $N_e$ unidirectional composite layers, and the thickness of each layer is described by a polynomial in $x$ and $y$ of the form

$$t_{il}(x, y) = \sum_{it=1}^{Itl} T_{(il,it)} \cdot x^{mt(il,it)} \cdot y^{nt(il,it)} \tag{2}$$

where $il$ is the index for the $il$th layer, and $it$ is the index for the $it$th term in the thickness polynomial of the $il$th layer. The coefficients $T(il, it)$ define the thickness of the $il$th layer. They serve as sizing design variables for that layer. The exponents $mt(il, it)$, $nt(il, it)$ are preassigned and can be selected

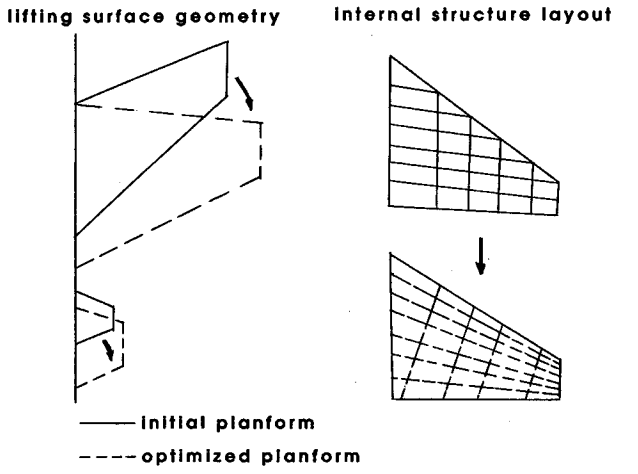


**Fig. 1 Planform shape variation of lifting surfaces and their internal structure.**

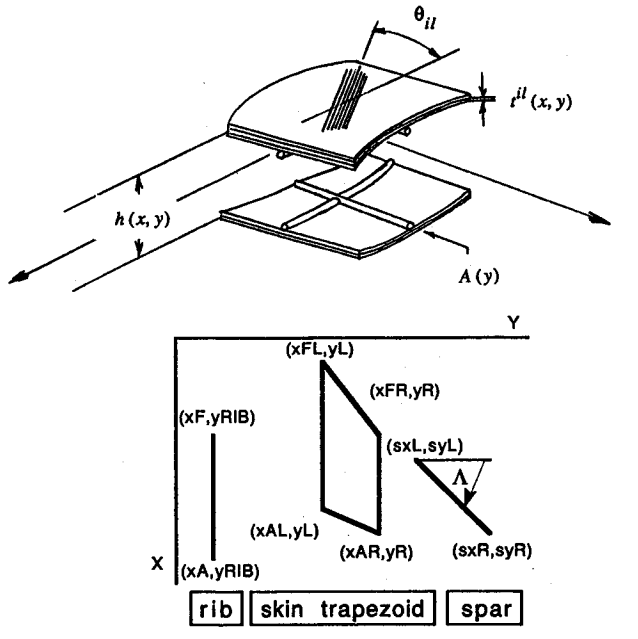


**Fig. 2 Shape design variables for wing trapezoids, spars, and ribs.**

to generate a complete polynomial or to represent a product of a polynomial in $x$ by a polynomial in $y$.[4,9]

Cap area for spars and ribs are allowed to vary linearly. In the case of a spar, the cap area $A^S$ is defined in term of the spanwise coordinate $y$, and in the case of a rib, the cap area $A^R$ is a function of $x$:

$$A^S(y) = A_1^S + A_2^S y \tag{3}$$

$$A^R(x) = A_1^R + A_2^R x \tag{4}$$

The coefficients $A_i^R$ and $A_i^S$ serve as sizing type design variables for the cap areas.

Other elements include translational and rotational springs and concentrated masses. Springs connect points on the planform to each other or to the ground. They can be used to enforce boundary conditions such as zero transverse displacement or zero slope in a given direction if their stiffness is high enough. They can also serve to connect major wing segments, such as control surfaces and a wing box, to each other.[4,9] Concentrated masses placed in an array of points over the wing are used to represent nonstructural items.

## Stiffness and Mass Matrix Terms

Elements of the stiffness and mass matrices are linear in the sizing design variables $T(il, it)$, $A_i^S$ and $A_i^R$. They are also linear combinations of members of certain families of area and line integrals, as shown in the following. It is beyond the scope of this article to describe in detail the derivation of mass and stiffness contributions from all structural elements in the model. Key steps in these derivations and important features of the formulation are discussed, however, by focusing on the contribution of skin layers.

Let wing displacements in the $x$, $y$, and $z$ directions be

$$\{U(x, y, z, t)\}^T = \{u, v, w\} \tag{5}$$

The plane of symmetry for a symmetric depth distribution is taken to be $z = 0$. Classical plate theory (CPT) simplifies the kinematics by expressing the in-plane displacements in terms of the vertical displacement $w(x, y, t)$ as follows:

$$u = -zw_{,x} = -z\frac{\partial w}{\partial x}$$

$$v = -zw_{,y} = -z\frac{\partial w}{\partial y} \tag{6}$$

Cover skins are assumed thin with respect to the depth of the wing, and their initial curvature negligible. Plies with identical fiber direction are lumped into layers, and the thickness distribution of the $il$th layer corresponds to the $il$th fiber direction [Eq. (2)]. For skin layers in a state of plane stress, the stress-strain relations for the $il$th layer in global (off-axis) coordinates $x$, $y$ are

$$\{\sigma^{il}\} = [Q^{il}]\{\varepsilon\} \tag{7}$$

where the engineering strains are

$$\{\varepsilon\}^T = \{\varepsilon_{xx}, \varepsilon_{yy}, \gamma_{xy}\} \tag{8}$$

and the stresses in the $il$th layer are

$$\{\sigma^{il}\}^T = \{\sigma_{xx}, \sigma_{yy}, \sigma_{xy}\} \tag{9}$$

Substituting Eqs. (6) into Eq. (8) to express the strains in terms of displacements, and replacing $z$ by $h/2$ (the location of an infinitesimal skin element above the wing reference plane), make it possible to express the skin contribution to the strain energy of the wing (including lower and upper skins) in the form

$$PE = \sum_{il=1}^{Nl} \int_x \int_y t_{il}(x, y)\frac{h^2(x, y)}{4}[w_{,xx}, w_{,yy}, 2w_{,xy}][Q^{il}] \times \begin{bmatrix} w_{,xx} \\ w_{,yy} \\ 2w_{,xy} \end{bmatrix} dx\, dy \tag{10}$$

To complete the formulation in terms of simple polynomial series, the Ritz functions for the out-of-plane displacement $w(x, y, t)$ are selected as

$$w(x, y, t) = \sum_{i=1}^{nq} x^{mw(i)} y^{nw(i)} q_i(t) \tag{11}$$

where the exponents $mw(i)$ and $nw(i)$ associated with the $i$th Ritz function are preassigned. Again, complete polynomials can be used and boundary conditions imposed by using stiff springs. Alternatively, polynomial terms can be selected in a way that automatically satisfies boundary conditions.[4,9]

The skin in-plane engineering strains are obtained from the vector of curvatures

$$\begin{bmatrix} w_{,xx} \\ w_{,yy} \\ 2w_{,xy} \end{bmatrix} = [W(x, y)]\{q(t)\} \tag{12}$$

where $[W(x, y)]$ is a $3 \times nq$ matrix whose elements are polynomial terms [Eqs. (11) and (12)] shown in Eq. (13) (elements of the $j$th column are shown):

$$[W(x, y)] = \begin{bmatrix} \cdots & \cdots & mw(j)(mw(j) - 1)x^{mw(j)-2}y^{nw(j)} & \cdots & \cdots & \cdots \\ \cdots & \cdots & nw(j)(nw(j) - 1)x^{mw(j)}y^{nw(j)-2} & \cdots & \cdots & \cdots \\ \cdots & \cdots & 2mw(j)nw(j)x^{mw(j)-1}y^{nw(j)-1} & \cdots & \cdots & \cdots \end{bmatrix} \tag{13}$$

Note that if any of the exponents $mw(j) - 1$, $mw(j) - 2$, $nw(j) - 1$, or $nw(j) - 2$ is less than 0 (as a result of differentiating constant or first-order terms), then the corresponding term in the $W(x, y)$ matrix is 0.

Realizing that $W(x, y)$ is a matrix of polynomial terms, let the $k, l$ element of the matrix $W(x, y)$ be written as

$$W_{k,l}(x, y) = \bar{W}(k, l)x^{MW(k,l)}y^{NW(k,l)} \tag{14}$$

Each $W_{k,l}$ is stored (for computational purposes) as a coefficient and two exponents. $\bar{W}(k, l)$ is the coefficient corresponding to element $k, l$. $MW(k, l)$ is the power of $x$ in the $k, l$ term, and $NW(k, l)$ is the power of $y$ in the $k, l$ term.

We substitute Eq. (12) into Eq. (10) to get an expression of the potential energy in terms of the generalized displacements $\{q\}$

$$PE = \{q\}^T \left( \sum_{il=1}^{Nl} \int_x \int_y t_{il}(x, y) \frac{h(x, y)^2}{4} \times [W(x, y)^T][Q^{il}][W(x, y)] \, dx \, dy \right) \{q\} \tag{15}$$

We now substitute the polynomial series for $h(x, y)$, $t_{il}(x, y)$ and $W(x, y)$ [Eqs. (1), (2), and (14)], and carry out the matrix multiplications and area integration. The $i, j$ term of the skin contribution to the stiffness matrix (assuming symmetry of upper and lower skins with respect to $z = 0$) is

$$K(i, j) = 2 \sum_{il=1}^{Nl} \sum_{it=1}^{Itl} \sum_{ih=1}^{N_H} \sum_{jh=1}^{N_H} \sum_{k=1}^{3} \sum_{l=1}^{3} T(il, it)H(ih)H(jh) \times \bar{W}(k, i)\bar{W}(l, j)Q^{il}(k, l) \cdot \frac{1}{4} \int_x \int_y x^r y^s \, dx \, dy \qquad i = 1, nq, \quad j = 1, nq \tag{16}$$

where the exponents of $x$ and $y$ in the integrand are obtained as sums of exponents from the polynomial series for thickness, depth, and from Ritz functions in the matrix $[W(x, y)]$:

$$r = mt(il, it) + mh(ih) + mh(jh) + MW(k, i) + MW(l, j)$$
$$s = nt(il, it) + nh(ih) + nh(jh) + NW(k, i) + NW(l, j) \tag{17}$$

The contribution of skin layers to the stiffness of the wing is then a linear combination of elements of a family of area integrals of the form

$$I_{TR}(r, s) = \int_x \int_y x^r y^s \, dx \, dy \tag{18}$$

The area integration is carried out over the different trapezoids defining the planform. When loading of the wing is continuous and is described by a polynomial pressure over the wing, then the generalized loads are also linear functions of area integrals from the family in Eq. (18). In a similar manner all contributions to the mass matrix from skin layers are linear combinations of the same area integrals.

When depth, thickness, cap area, and Ritz polynomials are all given in global coordinates $(x, y)$, it is possible to obtain analytic expressions for the contributions of spar and rib caps to the stiffness and mass matrices. In the case of the spar, the derivation is similar to that for the skin, except that integration is done along the spar line, and finally $x$ in all polynomial terms is replaced by the spar line equation (defining the location of points along the spar line in the $x$-$y$ reference plane)

$$x(y) = S_1 y + S_2 \tag{19}$$

All stiffness and mass terms due to spar cap contribution are linear combinations of line integrals of the form

$$I_{SP}(m, n) = \int_0^L x^m(\eta)y^n(\eta) \, d\eta \tag{20}$$

evaluated along the length of the spar from 0 to $L$. When transformed into integration with respect to $y$, these integrals become

$$I_{SP}(m, n) = \frac{1}{\cos \Lambda} \int_{y_L}^{y_R} (S_1 y + S_2)^m y^n \, dy \tag{21}$$

where $\Lambda$ is the spar's sweep angle (Fig. 2). Similarly, each rib contribution is linearly dependent on a family of line integrals along the rib axis from the rib's front edge at $xF$ to its rear edge at $xA$

$$I_{RB}(m, n) = y_{RIB}^n \cdot \int_{xF}^{xA} x^m \cdot dx \tag{22}$$

where $y_{RIB}$ defines the spanwise location of the rib.

Each of these families of integrals depends on planform geometry. In the following section the area integrals are addressed and expressions for their shape sensitivities are derived. Spar and rib integrals and their shape sensitivities are obtained in a similar manner.

## Evaluation of the Area Integrals

Equations for the front line and aft line of a trapezoid can be written as

$$xf(y) = f_1 \cdot y + f_2 \tag{23}$$

$$xa(y) = a_1 \cdot y + a_2 \tag{24}$$

where $a_1, a_2, f_1$, and $f_2$ are explicit functions of the trapezoid's planform shape design variables $y_L$, $y_R$, $x_{FL}$, $x_{FR}$, $x_{AL}$, $x_{AR}$. The integral $I_{TR}$ can now be written as

$$I_{TR}(m, n) = \int_{y_L}^{y_R} y^n \int_{xf(y)}^{xa(y)} x^m \, dx \, dy \tag{25}$$

Using Equations (23) and (24) we get

$$\int_{xf(y)}^{xa(y)} x^m \, dx = \frac{1}{(m + 1)} [(a_1 \cdot y + a_2)^{m+1} - (f_1 \cdot y + f_2)^{m+1}] \tag{26}$$

and then Eqs. (25) and (26) yield

$$I_{TR}(m, n) = \frac{1}{(m+1)}[I_A(n, m+1) - I_F(n, m+1)] \tag{27}$$

where two new families of line integrals in $y$ are defined as

$$I_A(r, s) = \int_{y_L}^{y_R} y^r(a_1 \cdot y + a_2)^s \, dy \tag{28}$$

$$I_F(r, s) = \int_{y_L}^{y_R} y^r(f_1 \cdot y + f_2)^s \, dy \tag{29}$$

Recall [Eq. (21)] that spar line integrals are also of the same form, with the line coefficients $f_1$ and $f_2$ replaced by $S_1$ and $S_2$ for the spar. Several recursion formulas are available for evaluating these integrals (see Ref. 18, p. 61), and tables of integrals for each trapezoid, spar and rib are generated and stored before assembly of stiffness and mass matrices starts. The family of area integrals $I_{TR}(m, n)$ is generated for each trapezoid, with $m$ and $n$ varying from 1 to $m$(max) and $n$(max) as dictated by the order of polynomials used for thickness, depth, and Ritz functions. Thus, stiffness and mass matrix terms due to skins, spars, and ribs are obtained based on analytic integrations over the trapezoids, and no numerical integration is needed.

## Shape Sensitivities of the Area Integrals

Since the area integrals are linear in terms of members of the families of line integrals $I_A$ and $I_F$ [Eq. (27)], shape sensitivities of these line integrals are needed for calculating sensitivities of stiffness and mass terms. Using Leibnitz's rule for the derivatives of definite integrals along with chain rule differentiation, we obtain

$$\frac{\partial I_F(r, s)}{\partial y_R} = y_R^r \cdot (f_1 \cdot y_R + f_2)^s + s\frac{\partial f_1}{\partial y_R} \cdot \int_{y_L}^{y_R} y^{r+1}(f_1 \cdot y + f_2)^{s-1} \, dy + s\frac{\partial f_2}{\partial y_R} \cdot \int_{y_L}^{y_R} y^r(f_1 \cdot y + f_2)^{s-1} \, dy \tag{30}$$

Note that $f_1$ and $f_2$ are explicitly dependent on $y_R$, and that the integrals in Eq. (30) are already available from the family of integrals $I_F(r, s)$ [Eq. (29)] generated for the analysis of the wing structure. The derivative of $I_F$ with respect to $y_L$ is obtained in a similar manner. Derivatives of the $I_F$ and $I_A$ integrals with respect to any $x$ coordinate of an edge ($x_{FL}$, $x_{FR}$, $x_{AL}$, $x_{AR}$) are also obtained by analytic differentiation of the line integrals. This time, however, the integration limits ($y_L$, $y_R$) do not depend on the design variables and the derivatives are simpler. If $x_{ij}$ is any of the four $x$ coordinates of an edge point, then

$$\frac{\partial I_F(r, s)}{\partial x_{ij}} = s\frac{\partial f_1}{\partial x_{ij}} \cdot \int_{y_L}^{y_R} y^{r+1}(f_1 \cdot y + f_2)^{s-1} \, dy + s\frac{\partial f_2}{\partial x_{ij}} \cdot \int_{y_L}^{y_R} y^r(f_1 \cdot y + f_2)^{s-1} \, dy \tag{31}$$

Of course, since $I_F$ does not depend on the geometry of the aft line

$$\frac{\partial I_F}{\partial x_{AL}} = 0 \tag{32}$$

$$\frac{\partial I_F}{\partial x_{AR}} = 0 \tag{33}$$

Analytic shape sensitivities of the $I_A$ integrals are obtained in a similar manner. Again, it is found out that they are linear combinations of members of the family $I_A(r, s)$ that are already available from the analysis phase. No new integrations are then needed for the sensitivity derivatives of stiffness and mass terms.

## Geometry of Output Points (Output Grid)

While the analytic derivatives of area and line integrals described in the previous section make it possible to obtain analytical derivatives of stiffness and mass terms, it should be remembered that when a planform shape is varied, the grid points used for evaluation of stresses and displacements also move. This motion of an output point contributes to the shape sensitivity of displacement and stresses at that point.[19]

A Ritz polynomial series is used for the displacements in the equivalent plate approach used here.[2,3,8,9] Thus, at an output point on the planform $(x_0, y_0)$ the displacement is given by [Eq. (11)]

$$w(x_0, y_0) = \sum_{i=1}^{N_w} x_0^{mw(i)} y_0^{nw(i)} q_i \tag{34}$$

In the case of a static solution, the vector of generalized displacements $\{q\}$ is obtained from the solution of the matrix equation

$$[K] \cdot \{q\} = \{Q\} \tag{35}$$

where $[K]$ is the generalized stiffness matrix, and $\{Q\}$ is the generalized load vector. If $p$ is a shape design variable, then the vector of derivatives $(\partial\{q\})/(\partial p)$ depends only on the shape derivatives of $[K]$ and $\{Q\}$. However, the displacement at $(x_0, y_0)$ depends also on the derivatives $(\partial x_0)/(\partial p)$ and $(\partial y_0)/(\partial p)$.

Figure 3 shows a transformation between a reference grid, defined on a unit square, and the physical grid on a trapezoid. The grid determines an array of points where stresses and displacements are evaluated. The wing trapezoid for output purposes (to be named "output panel") does not have to coincide with a structural trapezoid.

The transformation of a point from the reference grid $(\zeta, \eta)$ to its physical location $(x, y)$ depends on the planform geometry of the output panel, which is defined, similar to the structural panel, by a design variable vector of six shape design variables

$$\{x^{OP}\}^T = (y_L, y_R, x_{FL}, x_{FR}, x_{AL}, x_{AR}) \tag{36}$$

We now define the following matrices

$$[F] = \begin{bmatrix} 1 & \zeta & \eta & \zeta\eta & 0 & 0 \\ 0 & 0 & 0 & 0 & 1 & \eta \end{bmatrix} (2 \times 6) \tag{37}$$

$$[G] = \begin{bmatrix} [G_{11}] & [G_{12}] \\ [G_{21}] & [G_{11}^T] \end{bmatrix} (6 \times 6) \tag{38}$$

where

$$[G_{11}] = \begin{bmatrix} 0 & 0 \\ 0 & 0 \\ 0 & 0 \\ 0 & 0 \end{bmatrix} \tag{39}$$

$$[G_{12}] = \begin{bmatrix} 1 & 1 & 1 & 1 \\ -1 & -1 & 1 & 1 \\ -1 & 1 & -1 & 1 \\ 1 & -1 & -1 & 1 \end{bmatrix} \tag{40}$$

$$[G_{21}] = \begin{bmatrix} 2 & 2 \\ -2 & 2 \end{bmatrix} \tag{41}$$

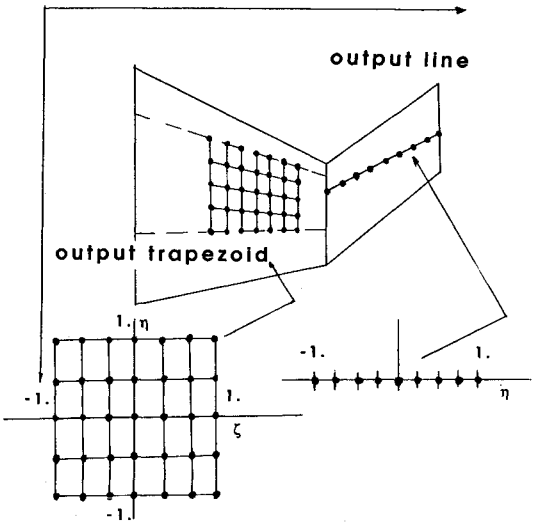


**Fig. 3 Geometry of output panels and output lines.**

The $(x, y)$ coordinates of a point $(\zeta, \eta)$ are obtained as follows:

$$\begin{bmatrix} x \\ y \end{bmatrix} = [F(\zeta, \eta)] \cdot [G] \cdot \{x^{OP}\} \tag{42}$$

It is clear, then, that $(x_0, y_0)$ of a given grid point $(\zeta, \eta)$ is linearly dependent on the trapezoidal shape design variables defining the output panel. As this output panel changes shape and moves, the point $(x_0, y_0)$ moves. The derivatives $(\partial x_0)/(\partial p)$ and $(\partial y_0)/(\partial p)$, $(p \in \{x^{OP}\})$ are now easy to obtain from Eq. (42). The sensitivity of the displacement with respect to a shape design variable $p$ at a point, in the case where the output panel and structural panel coincide (same six shape design variables for both), is [see Eq. (34)]

$$\frac{\partial w(x_0, y_0)}{\partial p} = \sum_{i=1}^{N_w} \left\{ x_0^{mw(i)-1} y_0^{nw(i)} q_i \cdot mw(i) \cdot \frac{\partial x_0}{\partial p} + x_0^{mw(i)} y_0^{nw(i)-1} q_i \cdot nw(i) \cdot \frac{\partial y_0}{\partial p} + x_0^{mw(i)} y_0^{nw(i)} \cdot \frac{\partial q_i}{\partial p} \right\} \tag{43}$$

where $(\partial\{q\})/(\partial p)$ is obtained from[1]

$$[K] \frac{\partial \{q\}}{\partial p} = \left\{ \frac{\partial Q}{\partial p} \right\} - \frac{\partial [K]}{\partial p} \{q\} \tag{44}$$

Stress shape sensitivities are obtained in a similar manner.

## Test Case

The fighter wing model presented in Ref. 3 is used here for all numerical studies. It is cantilevered along the root chord and subject to a uniform 1 psi pressure load over its planform surface. Two types of planform shape variation are studied. In the first case, the root and tip chords are fixed in global coordinates, and the chord connecting inner and outer wing trapezoids is moved in the $x$ direction (Fig. 4). In the second case, the wingtip is moved in the $x$ direction (no span change), changing the sweep of the outer wing section. Displacements and stresses are evaluated at the center point of the outer wing. This point moves as the planform changes, and thus structural behavior at this point varies due to stiffness and load changes as well as due to the movement of the point itself. Natural frequencies and mode shapes are also calculated. Behavior sensitivities with respect to the change in shape are obtained both analytically (using the technique described in previous sections), by first-order forward finite differences and by central differences. For most of the calculations, a single Ritz polynomial is used for the displacements over the whole wing. It is a complete polynomial without the terms of the form $x^i$ or $x^i y$, to impose the cantilever boundary condition along the root chord at $y = 0$. All computations were carried out on a HP Apollo 800 workstation in extended precision.

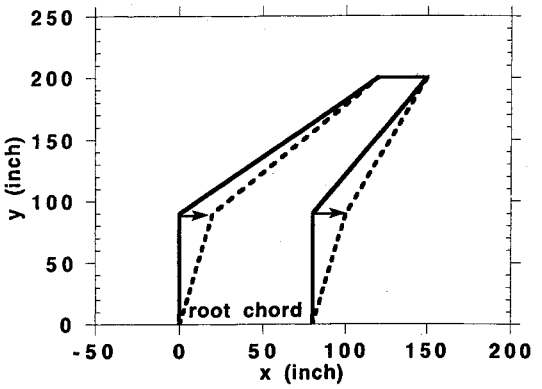


**Fig. 4 Planform of the fighter wing[3] and its shape variation.**

## Results

### Analysis Convergence

Poor conditioning with simple polynomials and the breakdown of the analysis when polynomial order is too high[3,9] are major problems in the equivalent plate modeling using ELAPS and LS-CLASS. Since the number of Ritz functions used cannot be increased beyond a certain limit, there is a difficulty in obtaining converged analysis results. It is then difficult to know what order of a Ritz function series should be used to obtain results that will be accurate enough for the purpose of preliminary design. Of course, it is always advisable to use a baseline test case to compare equivalent plate and finite element results.[3,4,20] The Ritz polynomials found suitable for good correlation can then be used for shape variations of the baseline wing without the need for finite element analysis of each new shape.

In Figures 5 and 6 we examine the convergence of typical normalized displacement, stress and natural frequency and their derivatives with respect to shape. The wingtip moves in the $x$ direction without change in span or tip chord. A "zoning" technique is used in the cases leading to Figs. 5 and 6.[9,20] As we have already seen, the wing planform is made of trapezoidal areas for the purpose of obtaining analytical expression for stiffness and mass integrals. The planform can also be broken into "zones." Each zone can contain several area trapezoids.

Separate Ritz function series are used for the different zones. Therefore, compatibility of displacement and slope is guaranteed inside a zone, but not between zones. Separate zones are connected to each other via linear and rotational springs to impose deformation compatibility or to represent known local discontinuities such as the attach line between a control surface and a wing box.[9,20] Zoning enables us not only to deal with geometric discontinuities in the wing. In addition, zones can also make it possible to reduce the order of Ritz polynomials needed, if enough of them are used. With zones, the Ritz analysis in the equivalent plate technique resembles the $p$ version of the finite element method.

In Fig. 5 we follow the behavior of typical normalized displacement, stress, and natural frequency for a case of one zone (one Ritz series for the whole wing) and a case of two zones (separate Ritz series for the inner and outer wings). Polynomial order was varied from 4 to 7. Although converged results are not guaranteed, it is clear in the cases of displacement and natural frequency that with 2 zones and polynomial order of 5, results are within 3% of the 2 zone/order 7 results. Similar predictions of displacement and natural frequency are available with a 1 zone/order 7 polynomial, and 2 zone/order

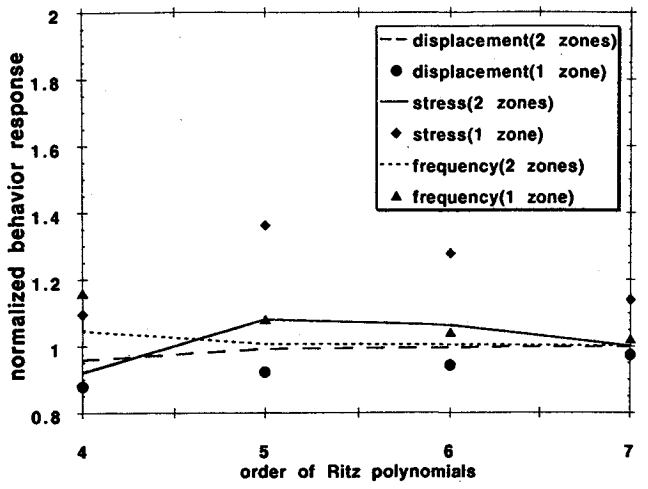


Fig. 5 Convergence of typical normalized displacement, stress, and natural frequency.

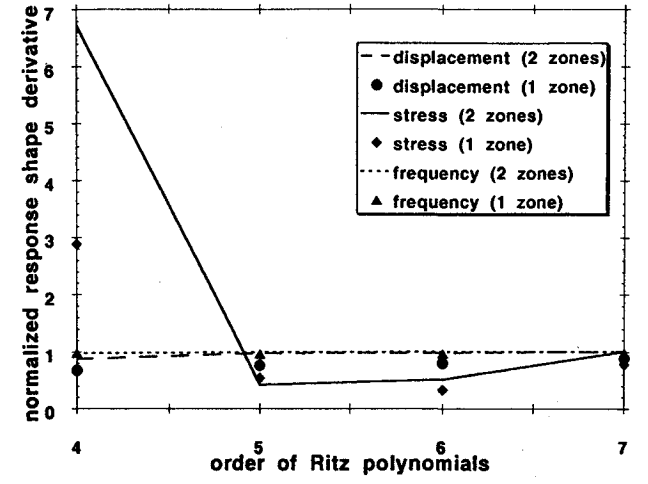


Fig. 6 Convergence of displacement, stress, and natural frequency shape sensitivities.

5 polynomial Ritz series. The convergence of the analytic shape derivatives is shown in Fig. 6. Again, with 2 zones and order 5 polynomials, displacement and frequency derivatives are practically converged. So are the results obtained with 1 zone/order 7, although there is a difference of about 10% in the displacement derivative.

The stress is more problematic, as expected. Smaller variation in stress value as the order of polynomials increases can be observed in Fig. 5 for the 2 zone case compared with the 1 zone case. The result obtained with a 1 zone/order 7 solution is within 6% of the result with 2 zones/order 5.

### Sensitivity Derivatives

The effect of step size on the accuracy of first-order forward finite difference derivatives of a typical displacement is shown in Fig. 7. In the following cases the planform shape variation is shown in Fig. 4. Results are obtained for a single zone and Ritz polynomial series of order 5 (10 terms) to order 7 (21 terms). As expected, accuracy of the finite difference derivative suffers when the step size is too small (roundoff error) and when it is too large (truncation error, Ref. 1, pp. 256–259). When the order of the Ritz series is increased and the system becomes more poorly conditioned, there is a wider range of step sizes leading to large errors in the finite difference derivative. The range of acceptable step sizes, then, narrows considerably. Figure 8 shows errors in finite difference derivatives with respect to the planform shape of a typical Tsai-Wu equivalent stress (normalized). With 21 terms in the

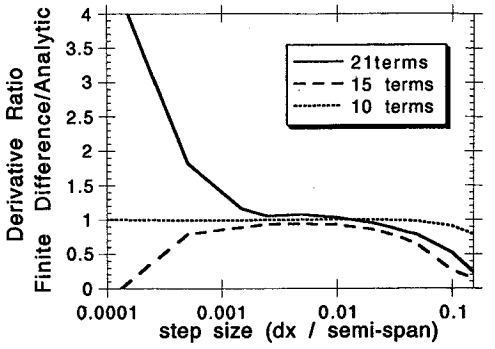


Fig. 7 Errors in first-order finite difference displacement sensitivities with respect to shape (single zone).

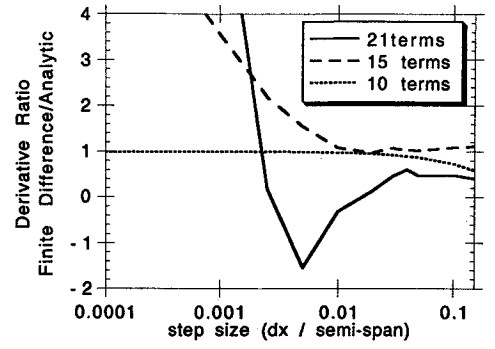


Fig. 8 Errors in first-order finite difference stress sensitivities with respect to shape (single zone).

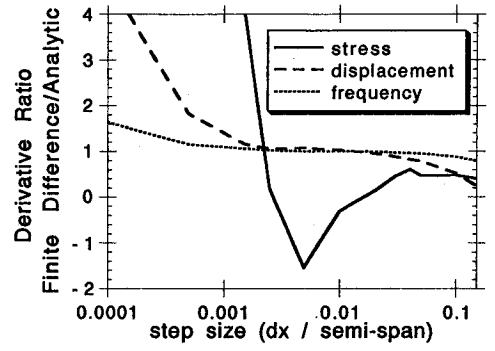


Fig. 9 Errors in first-order finite difference displacement, stress, and natural frequency sensitivities with respect to shape (single zone, seventh-order Ritz polynomials used).

Ritz series (order 7) there is no step size that yields acceptable finite difference results. Figure 9 shows errors in the finite difference derivatives of typical normalized displacement, stress, and natural frequency for the case with a single zone and a seventh-order Ritz series. Again, it is clear that due to ill conditioning and the resulting large roundoff errors, there is no range of step sizes leading to acceptable results. It should be emphasized that the analysis results themselves (the values of displacement, stress, and natural frequency) are still good in this case, despite the poor conditioning of the static and eigenvalue problems.

Using central differences instead of first-order forward differences does not solve the problem. While significant improvement is obtained in the cases of displacement and natural frequency responses, the central difference stress derivative (in the case of single zone, seventh-order Ritz polynomial) is still subject to considerable errors (Fig. 10). It is also interesting to note that when first-order finite difference differentiation is carried out with respect to a sizing type design variable (in this case, the thickness of the skin) the accuracy

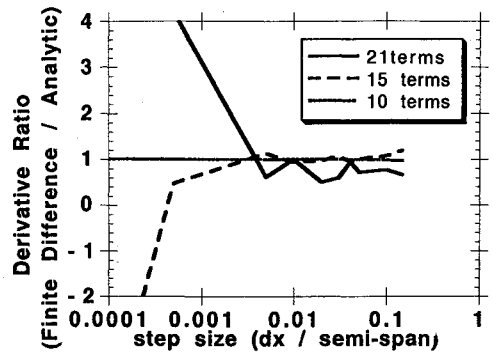


**Fig. 10 Errors in central difference stress sensitivities with respect to shape (single zone).**

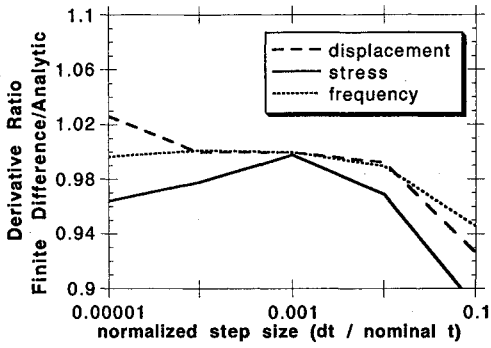


**Fig. 11 Errors in first-order finite difference displacement, stress, and natural frequency sensitivities with respect to sizing (single zone, seventh-order Ritz polynomials used).**

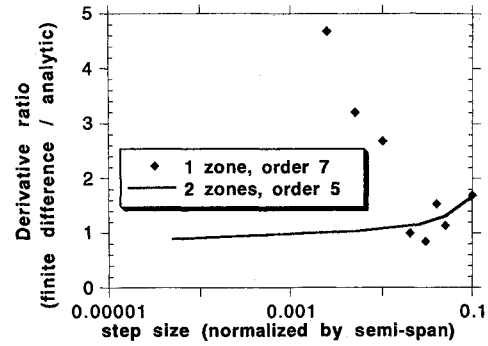


**Fig. 12 Effect of zoning on first-order finite difference stress shape derivative.**

problems just described are much less severe (Fig. 11). As a matter of fact, in the sizing case with a seventh-order Ritz series, it is possible to obtain first-order finite difference derivatives with an error of less than 3%, compared with the analytic derivatives for quite a wide range of step sizes.

Analytic shape sensitivities are thus extremely important with equivalent plate wing models based on simple polynomial Ritz series because of the poor numerical conditioning of the resulting equations, and the nonlinear dependence of stiffness and mass terms on the shape design variables (as compared to the linear dependence on sizing type design variables).

Since equivalent analysis results can be obtained in the present case with a 1 zone/order 7 and a 2 zone/order 5 solutions, it is tempting, when finite difference derivatives are needed, to turn to the solution that is less ill conditioned. Figure 12 shows the effect of step size on the first-order finite difference shape derivative for the moving tip case. While, as in Fig. 8, there is only a very narrow range of step sizes that leads to acceptable accuracy in the more ill conditioned case of 1 zone/order 7, it is clear that quite good finite difference derivatives are available for a wide range of step sizes for the better conditioned 2 zone/order 5 case.

Zoning, then, can help reduce the order of Ritz polynomials used for the analysis to produce equations that are less ill conditioned, and lead to reliable finite difference shape derivatives.

## Conclusions

Equations for calculating analytical derivatives of structural wing response with respect to wing planform shape design variables were derived. These analytical sensitivities are general and can be used with planform shape as well as rib and spar shape design variables. By proper organization of the analysis and sensitivity calculation processes, a computationally efficient equivalent plate wing modeling capability was developed. The analytical shape sensitivities were then used to check accuracy of finite difference sensitivities that are still needed with current wing plate models. In some cases, because of the poor conditioning of the governing equations, it is impossible to obtain accurate shape sensitivities based on first-order finite differences. Zoning (together with lower order Ritz polynomials in each zone) can improve the situation. However, accuracy problems are eliminated by the method presented herein for the efficient calculation of sensitivity derivatives. This new capability is a valuable extension to equivalent plate analysis procedures that are based on a simple polynomial Ritz formulation, especially when planform changes are being considered.

## Acknowledgments

This research was carried out with the support of NASA Grant NAG 2-723, Hiro Miura, Technical Monitor. The author thanks H. Miura for his support and encouragement.

## References

[1]Haftka, R. T., and Gurdal, Z., *Elements of Structural Optimization*, 3rd Revised and Expanded Edition, Kluwer Academic Publishers, Dordrecht, The Netherlands, 1992.

[2]Lynch, R. W., Rogers, W. A., and Brayman, W. W., "Aeroelastic Tailoring of Advanced Composite Structures for Military Aircraft," U.S. Air Force Flight Dynamics Lab., Rept. AFFDL-TR-76-100, April 1977.

[3]Giles, G. L., "Equivalent Plate Analysis of Aircraft Wing Box Structures with General Planform Geometry," *Journal of Aircraft*, Vol. 23, No. 11, 1986, pp. 859–864.

[4]Giles, G. L., "Further Generalization of an Equivalent Plate Representation for Aircraft Structural Analysis," *Journal of Aircraft*, Vol. 26, No. 1, 1989, pp. 67–74.

[5]Triplett, W. E., "Aeroelastic Tailoring Studies in Fighter Aircraft Design," *Journal of Aircraft*, Vol. 17, No. 7, 1980, pp. 508–513.

[6]Schweger, J., Sensburg, O., and Berns, H., "Aeroelastic Problems and Structural Design of a Tailless CFC Sailplane," 2nd International Symposium on Aeroelasticity and Structural Dynamics, Aachen, Germany, April 1985.

[7]Sensburg, O., Schmidinger, G., and Fullhas, K., "Integrated Design of Structures," *Journal of Aircraft*, Vol. 26, No. 3, 1989, pp. 260–270.

[8]Livne, E., "Integrated Multidisciplinary Optimization of Actively Controlled Fiber Composite Wings," Ph.D.Dissertation, Mechanical, Aerospace, and Nuclear Engineering Dept., Univ. of California, Los Angeles, Los Angeles, CA, 1990.

[9]Livne, E., Schmit, L. A., and Friedmann, P. P., "Design Oriented Structural Analysis for Fiber Composite Wings," Univ. of California, Rept. UCLA-ENG-88-36, Los Angeles, CA, Nov. 1988.

[10]Barthelemy, J.-F. M., Coen, P. G., Wrenn, G. A., Riley, M. F., Dovi, A. R., and Hall, L. E., "Application of Multidisciplinary Optimization Methods to the Design of a Supersonic Transport," NASA TM-104073, March 1991.

[11]Bohlman, J. D., Love, M. H., Barker, D. K., Rogers, W. A., and Psul, B. E., "Application of Analytical and Design Tools for Fighter Wing Aeroelastic Tailoring," *Proceedings of the AIAA/ASME/ASCE/AHS/ASC 33rd Structures, Structural Dynamics, and Materials Conference* (Dallas, TX), AIAA, Washington, DC, 1992, pp. 2652–2639 (AIAA Paper 92-2373).

[12]Bohlman, J. D., Eckstrom, C. V., and Weisshaar, T. A., "Static Aeroelastic Tailoring for Oblique Wing Lateral Trim," *Journal of Aircraft*, Vol. 27, No. 6, 1990, pp. 558–563.

[13]Barthelemy, J.-F. M., and Hall, L. E., "Automatic Differentiation as a Tool in Engineering Design," *4th USAF/AIAA Conference on Multidisciplinary Analysis and Optimization* (Cleveland, OH), AIAA, Washington, DC, 1992, pp. 424–432 (AIAA Paper 92-4743).

[14]Barthelemy, J.-F. M., and Bergen, F. D., "Shape Sensitivity Analysis of Wing Static Aeroelastic Characteristics," *Journal of Aircraft*, Vol. 26, No. 8, 1989, pp. 712–717.

[15]Kapania, R., Bergen, F., and Barthelemy, J., "Shape Sensitivity Analysis of Flutter Response of a Laminated Wing," *Proceedings of the AIAA/ASME/ASCE/AHS/ASC 30th Structures, Structural Dynamics, and Materials Conference* (Mobile, AL), AIAA, Washington, DC, 1989, pp. 920–932 (AIAA Paper 89-1267).

[16]Nam, C., "Aeroservoelastic Tailoring for Lateral Control Enhancement," Ph.D. Dissertation, Purdue Univ. (Univ. Microfilm International Order Number 9031368), West Lafayette, IN, 1990.

[17]Singhvi, S., and Kapania, R. K., "Analytical Shape Sensitivities and Approximations of Modal Response of Generally Laminated Tapered Skew Plates," *Proceedings of the AIAA/ASME/ASCE/AHS/ASC 33rd Structures, Structural Dynamics, and Materials Conference* (Dallas, TX), AIAA, Washington, DC, 1992, Pt. III, pp. 1264–1271 (AIAA Paper 92-2391).

[18]Spiegel, M. R., *Mathematical Handbook*, Schaum's Outline Series, McGraw-Hill, New York, 1968.

[19]Haug, E. J., Choi, K. K., and Komkov, V., "Design Sensitivity Analysis of Structural Systems," Academic Press, Orlando, FL, 1986, Chap. 3.

[20]Livne, E., Sels, R. E., and Bhatia, K. G., "Lessons Learned from Application of Equivalent Plate Structural Modeling to an HSCT Wing," AIAA Paper 93-1413, April 1993.